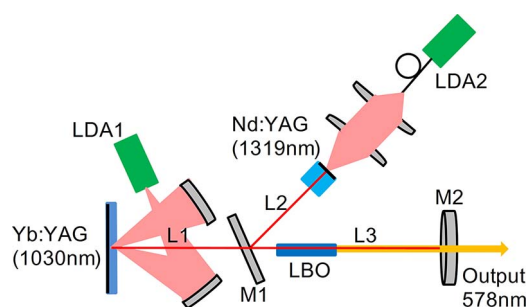


Generation of a 578-nm Yellow Laser by the Use of Sum-Frequency Mixing in a Branched Cavity

Volume 8, Number 1, February 2016

Jianming Yang
Huiming Tan
Yubing Tian
Wenming Yao
Gangfei Ma
Qiaojun Ju
Long Zhang
Jiansheng Chen
Zhi Li
Jing Gao



DOI: 10.1109/JPHOT.2016.2520820
1943-0655 © 2016 IEEE

Generation of a 578-nm Yellow Laser by the Use of Sum-Frequency Mixing in a Branched Cavity

Jianming Yang,^{1,2,3} Huiming Tan,¹ Yubing Tian,¹ Wenming Yao,¹
Gangfei Ma,^{1,3} Qiaojun Ju,^{1,4} Long Zhang,¹ Jiansheng Chen,¹
Zhi Li,¹ and Jing Gao¹

¹Jiangsu Key Laboratory of Medical Optics, Suzhou Institute of Biomedical Engineering and Technology, Chinese Academy of Sciences, Suzhou 215163, China

²Changchun Institute of Optics, Fine Mechanics and Physics, Chinese Academy of Sciences, Changchun 130033, China

³University of Chinese Academy of Sciences, Beijing 100049, China

⁴School of Electronic Engineering and Photo-Electric Technology, Nanjing University of Science and Technology, Nanjing 210094, China

DOI: 10.1109/JPHOT.2016.2520820

1943-0655 © 2016 IEEE. Translations and content mining are permitted for academic research only.

Personal use is also permitted, but republication/redistribution requires IEEE permission.

See http://www.ieee.org/publications_standards/publications/rights/index.html for more information.

Manuscript received December 16, 2015; revised January 15, 2016; accepted January 15, 2016. Date of current version February 3, 2016. This work was supported in part by the National Natural Science Foundation of China under Grant 61405236, by the 863 Program under Grant 2015AA021106, by the Natural Science Foundation of Jiangsu Province under Grant BK20131170, and by the Fundamental Research Project of Suzhou under Grant SYG201305 and Grant SYG201404. Corresponding author: J. Gao (e-mail: owengaojing@126.com).

Abstract: A compact, continuous-wave, solid-state laser at 578 nm has been demonstrated, for the first time to our knowledge, by use of intracavity sum-frequency mixing from a branched cavity with an LBO crystal. Two gain mediums, namely, the Nd:YAG single crystal and the Yb:YAG single crystal (with a disk laser setup), are used to generate the two fundamental 1319- and 1030-nm waves, respectively. The maximum output power of 37.5 mW is obtained at a total pump power of 14 W. The power stability value of the output laser is better than 4.3% in 30 min.

Index Terms: Solid-state lasers, diode-pumped lasers, visible lasers.

1. Introduction

The yellow laser source is widely used in the areas of medical science, including dermatology, ophthalmology, and super-resolution imaging. Today, the copper vapor laser (578 nm) and dye-lasers are commonly used in medical clinics for dermatological treatment [1]–[6], due to increased interaction between the photon and hemoglobin, which has high absorption peaks at 578 nm. Furthermore, the 578 nm laser has important applications in fundamental physics research and optical atomic clocks [7]–[11]. For Yb atom research, the hyperfine transitions of three iodine lines near the $^1S_0 \rightarrow ^3P_0$ transition of Yb at 578 nm could be important frequency reference lines [12]. In addition, narrow-linewidth 578 nm laser with high frequency stability has been used to probe the clock transition of ytterbium atoms confined in an optical lattice by several groups [9], [11], [13].

Compared with the copper vapor lasers and dye lasers, diode-pumped solid-state lasers have the advantages of small size, high efficiency, and none of the toxic gases and dyes used in the

laser [14], [15]. Up to now, different approaches have been used to produce solid-state laser at 578 nm. Lasers with sum-frequency generation (SFG) in a waveguide (WG) periodically poled lithium niobate (PPLN) device based on a 1319 nm Nd:YAG laser and a 1030 nm Yb-doped fiber laser were reported. The power level of this scheme was ~ 10 mW [8], [9], [13], which was rather low, due to the low damage threshold of the proton-exchange WG-PPLN. To improve the yellow laser power, a ridge-type WG-PPLN device was introduced into this scheme. As a result, a SFG power of ~ 150 mW was obtained [16]. However, the required narrow linewidth of the two independent fundamental frequency lasers and the lower optical damage threshold of the WG-PPLN limit the further power scaling of the 578 nm laser. In the case of pulsed operation with high peak power, intracavity frequency-doubled Raman laser was a promising approach. Q-switched output with as much as 1.2 W average power was obtained by using a diode-pumped Nd:YAG laser gain medium producing fundamental output at 1064 nm, an intracavity LiIO_3 Raman-active crystal that generates first-Stokes output at 1155 nm, and an intracavity LiB_3O_5 frequency-doubling crystal that producing 578 nm yellow light [17]. Furthermore, the second harmonic generation (SHG) of a laser diode can be an excellent alternative with a relatively low cost. A maximum yellow laser output power of more than 10 mW was demonstrated by employing a WG-PPLN device as the nonlinear medium for SHG of a laser diode at 1156 nm [7], [10], [18]. A high-efficiency optically pumped vertical-external-cavity surface-emitting laser (VECSEL) emitting watt-level at a wavelength around 578 nm was demonstrated by intracavity frequency doubling using a non-critically phase matched LBO crystal [19]. Till now, the way to generate a continuous wave (cw) 578 nm laser by intracavity SFG with dual-pumping and dual-cavity linked in a common arm has not been presented. This scheme incorporates the features of compactness, excellent power scalability and high beam quality. Moreover, benefiting from this scheme, the competition between the two fundamental frequency lasers is avoided, and the output mirror does not need to be precisely coated for the transmittance of the two fundamental frequency lasers.

In this paper, a compact 578 nm yellow laser is proposed and demonstrated using two separate cavities. The arms for sum-frequency mixing in these two cavities are overlapped. Two gain mediums are employed to generate two fundamental waves: Nd:YAG single crystal and Yb:YAG thin-disk crystal for generating 1319 nm and 1030 nm waves. In the common arm, sum frequency mixing is realized in a type-I critically phase matched (CPM) LBO crystal. With a total incident pump power of 14 W, a maximum output power of 37.5 mW at 578 nm is obtained. The stability of the yellow output is better than 4.3% in 30 min.

2. Experimental Setup

The experimental setup of the intracavity SFG of 578 nm laser is shown in Fig. 1. The separate pump source for different gain media used in our experiment was a fiber coupled laser diode arrays (LDA). LDA1 (diameter of 300 μm and numeral aperture of 0.22) emitting at the wavelength of ~ 940 nm was used to pump Yb:YAG disk crystal for 1030 nm oscillation. Considering the quasi-three-level characteristics of Yb:YAG crystal, thin-disk crystal and four-pass pump configuration which was achieved by a pair of high reflective mirrors were utilized. LDA2 (diameter of 200 μm and numeral aperture of 0.22) emitting at the wavelength of ~ 808 nm was employed as the end-pumping source for generating 1319 nm oscillation. Both of the central emission wavelengths of the pump sources could be changed by tuning the operative temperature to match the absorption peaks of the two kinds of laser gain medium.

One gain medium, a thin-disk 10 at.-%-doped Yb:YAG crystal with a diameter of 11 mm and a thickness of 0.42 mm was mounted with one face on a water-cooled copper heat sink. The pumping side of the Yb:YAG crystal was antireflection (AR) coated at 940 nm ($T > 99.6\%$) and 1030 nm ($T > 99.9\%$). The cooling side of the Yb:YAG crystal was high reflection (HR) coated at 940 nm and 1030 nm ($R > 99.9\%$). The other gain medium, that is, an a-cut Nd:YAG rod ($\Phi 5$ mm \times 6 mm) doped with 1 at.-% concentration of Nd^{3+} , was chosen in the experiment. The pumping side of the Nd:YAG was AR coated at 808 nm ($T > 95\%$) and HR coated at 1319 nm

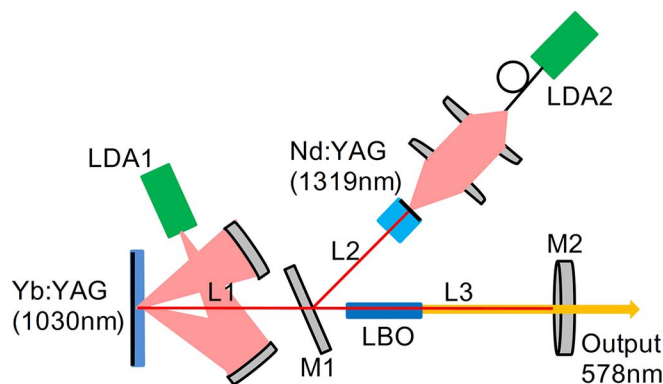


Fig. 1. Schematic of the intracavity SFG of 578 nm yellow laser.

($R > 99.9\%$). The opposite side was AR coated at 1319 nm ($T > 99.8\%$). A Type-I CPM LBO crystal ($3 \times 3 \times 10 \text{ mm}^3$, $\theta = 90^\circ$, $\varphi = 5^\circ$) was used to produce SFG at 578 nm. The LBO crystal was placed in a copper holder and the operative temperature at 27°C was maintained by a thermal electric cooler (TEC) with a precision of $\pm 0.1^\circ\text{C}$.

The experimental setup was constituted by a linear cavity for 1030 nm oscillation and a three-mirror folded cavity for the 1319 nm oscillation with a common arm (L3) which contained the SFG crystal. The pumping side of Nd:YAG crystal and the cooling side of Yb:YAG crystal acted as their own cavity mirrors, respectively. Mirror M1 which was HT coated at 1030 nm and 1064 nm ($T > 99.8\%$) on both sides and HR coated at 1319 nm ($R > 99.9\%$) on the right side played a role as a beam splitter for the two fundamental wavelengths, separating the cavity for the two laser crystal. M1 was designed HT at 1064 nm to suppress the more efficient transition line at 1064 nm in the Nd:YAG crystal. The output mirror (M2), which had a radius of curvature of 200 mm, was AR coated at 578 nm ($T > 96\%$) and HR coated at 1030 nm and 1319 nm ($R > 99.9\%$). The lengths of the two separate arms of the cavity (L1 and L2) were $\sim 73 \text{ mm}$ and $\sim 35 \text{ mm}$, respectively. The length of the common arm L3 was $\sim 42 \text{ mm}$. The value of the ratio ω_2/ω_1 in the present setup was ~ 1.05 , where ω_1 ($\sim 210 \mu\text{m}$) and ω_2 ($\sim 220 \mu\text{m}$) were the mode size in the LBO crystal for wavelengths 1319 nm and 1030 nm, respectively.

3. Results and Discussion

Fig. 2 depicts the characteristics of the cw output at 578 nm versus the absorbed pump power of Nd:YAG crystal and the pump power of Yb:YAG crystal. The pump thresholds of the yellow laser were measured to be $\sim 0.5 \text{ W}$ for the Nd:YAG laser and $\sim 2.2 \text{ W}$ for the Yb:YAG laser, respectively. The maximum yellow laser output power of 37.5 mW was obtained at a total pump power of 14 W. On this point, the pump power for Nd:YAG and Yb:YAG was 3.7 W and 10.3 W, respectively. The total yellow output power would be 75 mW if the lasers emitted in both the directions were taken into account. We notice that, at the efficient cw yellow laser operating, both the threshold and the pump power of the Yb:YAG laser was considerable high compared with the Nd:YAG laser. We attribute this result to two key points. One is the nature of Yb:YAG crystal, including the relative poor stimulated-emission cross section and the reabsorption of lower laser level according to the quasi-three-level characteristics of the Yb:YAG crystal [20]. The other is the inserting loss introduced by the beam splitter. The insertion loss can be estimated as $\sim 0.2\%$ according to the reflectance at 1030 nm of the beam splitter. The reflected laser power at 1030 nm from one side of the beam splitter as a function of the pump power of Yb:YAG laser is shown in Fig. 3. Though the two sides of the beam splitter were coated for high transmission at 1030 nm, we noticed that inserting loss introduced by the beam splitter could not be ignored. The reflection loss from one side was more than 0.25 W at the maximum yellow output condition. Moreover, we estimated that there was equivalent reflection loss taking

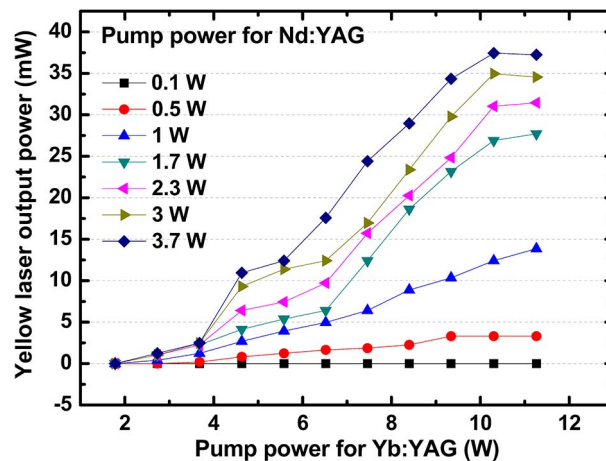


Fig. 2. Yellow output power versus the pump power for Nd:YAG crystal and the pump power for Yb:YAG crystal.

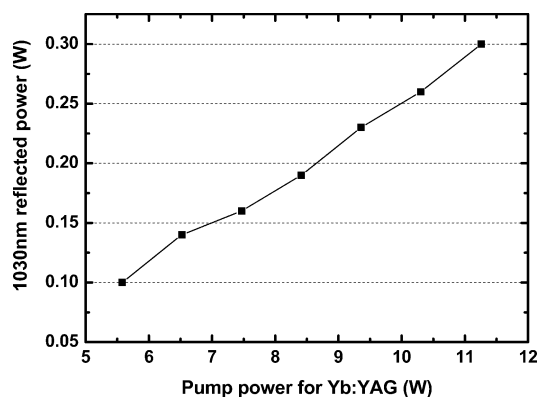


Fig. 3. Reflected power of 1030 nm versus the pump power for Yb:YAG crystal.

account of the coating curve, whereas it was inconvenient to measure the reflection loss from other side due to the cavity structure. In Fig. 2, there are several kinks in the output power lines when the Nd:YAG pump power is larger than 1 W. We ascribe this behavior to the competition between the neighboring 1319 nm and 1338 nm lines in the Nd:YAG laser. With lower Nd:YAG pump power, there was only one single line oscillating in the cavity. As the pump power increased, the other one would start oscillating and take part in the SFG process, resulting in these kinks.

A fiber spectrometer (Maya2000Pro, Ocean Optics, Inc.) with a resolution of ~ 1.1 nm (25 μm slit, HC-1 grating) was employed to monitor the yellow laser spectrum. As shown in Fig. 4(a), the optical spectrum of yellow laser at the maximum output power was not a single line but two lines. The highest intensity peak and the small peak nearby were located at 578 nm and 582 nm, respectively. When turned the azimuth angle of LBO, we obtained the maximum output power of 10 mW mainly at 582 nm under 14 W total pumping power with 3.7 W for Nd:YAG and 10.3 W for Yb:YAG. The corresponding spectrum was shown in Fig. 4(b). This indicated that there must be another spectral line taking part in the SFG generation. Another spectrometer (NIRQuest512, Ocean Optics, Inc.) with a resolution of ~ 2.0 nm (5 μm slit, 150 lines/mm blazed grating) was employed to monitor the infrared laser spectrum. The measured spectrum of 1338 nm laser is shown in the inset of Fig. 4(a). We conclude that the 1338 nm line was responsible for SFG of the 582 nm light. As a result, we did not get a single line at 578 nm at the

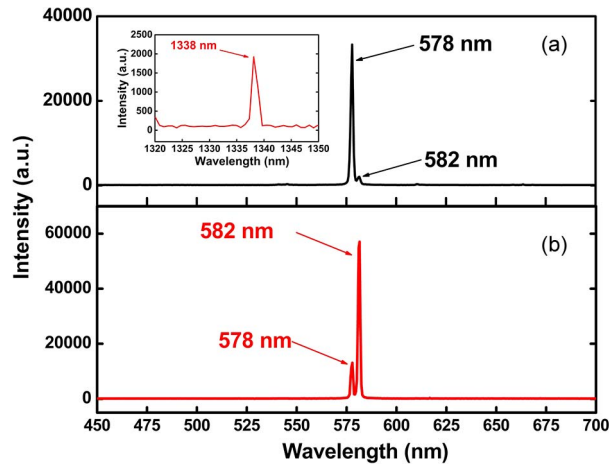


Fig. 4. Spectrum of the yellow laser. The inset is the spectrum of the 1338 nm laser.

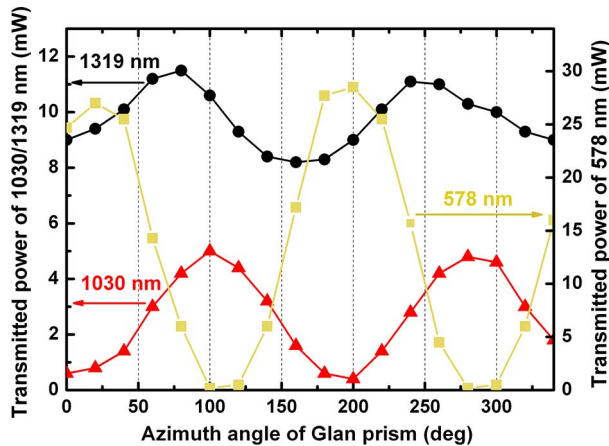


Fig. 5. Polarization measurement of 578 nm transmitted power from Glan prism (yellow squares), as well as 1030 nm power (red triangles) and 1319 nm power (black circles) without LBO as a function of the azimuth angle of Glan prism.

maximum output power. We assume there are two key points: first, the gain competition between the two lines was intense because the stimulated-emission cross sections of 1319 and 1338 nm are equivalent. For the Nd:YAG crystal, the stimulated-emission cross sections for $R_2 \rightarrow X_1$ (1319 nm) and $R_2 \rightarrow X_3$ (1338 nm) transitions are $0.92 \times 10^{-19} \text{ cm}^2$ and $0.90 \times 10^{-19} \text{ cm}^2$, respectively [21]. Second, it was difficult to discriminate the two lines by SFG because the spectral distance between the two lines was rather narrow. The exact conditions of the azimuth angle of the type-I critical phase matching LBO crystal for 578 nm and 582 nm are $\theta = 90^\circ$, $\varphi = 5^\circ$ and $\theta = 90^\circ$, $\varphi = 4.5^\circ$ at the same operative temperature, respectively. The maximum acceptance angle of LBO is 20 mrad for SFG of 1030 nm and 1319 nm, which is two times larger than the angle difference ($\Delta\varphi = 0.5^\circ$) between SFG of 578 nm and 582 nm.

Considering that the two gain media we employed were isotropic and the polarization states of the fundamental waves have a significant impact on the conversion efficiency of SFG, by using a Glan prism, we measured the polarization states of the 578 nm laser at the average output power of 31.5 mW, as well as the fundamental waves without the LBO crystal inside the cavity at the same pumping power. As shown in Fig. 5, the polarization states of 578, 1030, and 1319 nm lasers were *s*-polarized, approximate *p*-polarized and partially polarized, respectively. Because the beam splitter in the cavity acted as a polarizer for the 1030 nm laser, the

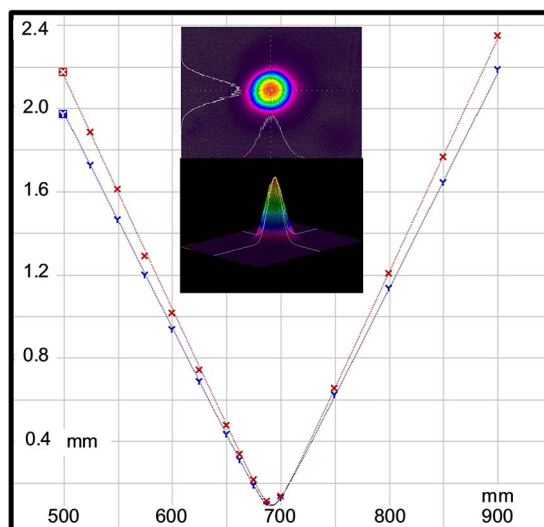


Fig. 6. Beam quality measurements of 578 nm yellow laser under the maximum output. (Inset) 2-D and 3-D spatial intensity profile.

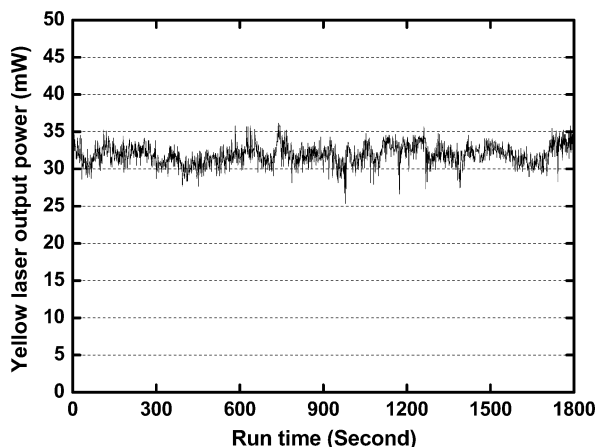


Fig. 7. Fluctuations of the 578 nm laser power at the average output of 31.5 mW.

polarization of 1030 nm laser well met the phase match condition. We believe that the SFG conversion efficiency will be dramatically enhanced if the polarization state of 1319 nm laser can be controlled, which can be simply done by inserting a Brewster plate inside the L3 arm of the cavity [22].

The transverse spatial profile of the 578 nm laser at the maximum output power was measured with the knife-edge method using a M^2 -200s-FW (Ophir-Spiricon, Inc.) laser beam analyzer. The M^2 factors were approximately 1.4 and 1.2 in the horizontal and vertical directions, respectively, which showed that the laser output at 578 nm was operating in the near TEM_{00} mode (Fig. 6). We considered that the asymmetry of the M^2 factors in the two directions was a result of the walk-off between the fundamental wave and the frequency mixed wave in the direction of LBO [23].

Finally, power stability of 578 nm laser was measured at the average output power of 31.5 mW. The power stability value of the output laser was better than 4.3% in the given 30 min. The fluctuation of the yellow laser output (see Fig. 7) in our experiment was largely due to the competition between the two laser lines at 1319 nm and 1338 nm.

4. Conclusion

A compact cw solid-state laser at 578 nm has been demonstrated, for the first time to our knowledge, by use of intracavity SFG from a branched cavity with two gain mediums and a type-I CPM LBO crystal. The maximum output power of 37.5 mW was obtained at 14 W of total pump power. We believe that further increase of the cw yellow output power would be a realistic goal by improving the utilization efficiency of 1030 nm laser and introducing the polarization control of 1319 nm laser. In addition, the linewidth and the frequency stability of the yellow laser deserve further investigation.

Acknowledgment

The authors are thankful for support from the Youth Innovation Promotion Association, CAS.

References

- [1] R. A. Neumann, R. M. Knobler, H. Leonhartsberger, and W. Gebhart, "Comparative histochemistry of port-wine stains after copper vapor laser (578 nm) and argon-laser treatment," *J. Invest. Dermatol.*, vol. 99, no. 2, pp. 160–167, Aug. 1992.
- [2] R. A. Sheehandare and J. A. Cotterill, "Copper vapour laser (578 nm) and flashlamp-pumped pulsed tunable dye laser (585 nm) treatment of port wine stains: Results of a comparative study using test sites," *Brit. J. Dermatol.*, vol. 130, no. 4, pp. 478–482, Apr. 1994.
- [3] R. A. Neumann, "Results and tissue healing after copper-vapour laser (at 578 nm) treatment of port wine stains and facial telangiectasias," *Brit. J. Dermatol.*, vol. 128, no. 3, pp. 306–312, Mar. 1993.
- [4] J. H. Chung, W. S. Koh, and J. L. Youn, "Histological responses of port wine stains in brown skin after 578 nm copper vapor laser treatment," *Lasers Surg. Med.*, vol. 18, no. 4, pp. 358–366, 1996.
- [5] N. S. Sadick and R. Weiss, "The utilization of a new yellow light laser (578 nm) for the treatment of class I red telangiectasia of the lower extremities," *Dermatol. Surg.*, vol. 28, no. 1, pp. 21–25, Jan. 2002.
- [6] H. I. Lee, "Clinicopathologic efficacy of copper bromide plus/yellow laser (578 nm with 511 nm) for treatment of melasma in Asian patients," *Dermatol. Surg.*, vol. 36, no. 6, pp. 885–893, Jun. 2010.
- [7] A. Y. Nevsky, "A narrow-line-width external cavity quantum dot laser for high-resolution spectroscopy in the near-infrared and yellow spectral ranges," *Appl. Phys. B*, vol. 92, no. 4, pp. 501–507, Sep. 2008.
- [8] S. Fang, "Coherence transfer from 1064 nm to 578 nm using an optically referenced frequency comb," *Chin. Phys. B*, vol. 24, no. 7, pp. 240–243, Jul. 2015.
- [9] C. W. Oates, "Stable laser system for probing the clock transition at 578 nm in neutral ytterbium," in *Proc. IEEE Conf. Int. Freq. Control Symp.-Jointly 21st Eur. Freq. Time Forum*, May 2007, vol. 1–4, pp. 1274–1277.
- [10] W. K. Lee, "Generation of 578 nm yellow light over 10 mW by second harmonic generation of an 1156 nm external-cavity diode laser," *Opt. Exp.*, vol. 19, no. 18, pp. 17453–17461, Aug. 2011.
- [11] M. Pizzocaro, "Realization of an ultrastable 578 nm laser for an Yb lattice clock," *IEEE Trans. Ultrason., Ferroelectr., Freq. Control*, vol. 59, no. 3, pp. 426–431, Mar. 2012.
- [12] F. L. Hong, H. Inaba, K. Hosaka, M. Yasuda, and A. Onae, "Doppler-free spectroscopy of molecular iodine using a frequency-stable light source at 578 nm," *Opt. Exp.*, vol. 17, no. 3, pp. 1652–1659, Feb. 2009.
- [13] Z. W. Barber, "Optical lattice induced light shifts in an Yb atomic clock," *Phys. Rev. Lett.*, vol. 100, no. 10, Mar. 2008, Art. ID 103002.
- [14] G. N. Tiwari, "Effect of addition of hydrogen to neon buffer gas of copper bromide vapor laser on its spectral and temporal characteristics," *Opt. Commun.*, vol. 338, pp. 322–327, Mar. 2015.
- [15] Q. Kou, I. Yesilyurt, and Y. Chen, "Collinear dual-color laser emission from a microfluidic dye laser," *Appl. Phys. Lett.*, vol. 88, no. 9, Feb. 2006, Art. ID. 091101.
- [16] K. Hosaka, "Evaluation of the clock laser for an Yb lattice clock using an optical fiber comb," *IEEE Trans. Ultrason., Ferroelectr., Freq. Control*, vol. 57, no. 3, pp. 606–612, Mar. 2010.
- [17] H. M. Pask and J. A. Piper, "Efficient all-solid-state yellow laser source producing 1.2 W average power," *Opt. Lett.*, vol. 24, no. 21, pp. 1490–1492, Nov. 1999.
- [18] E. B. Kim, W. K. Lee, C. Y. Park, D. H. Yu, and S. E. Park, "Narrow linewidth 578 nm light generation using frequency-doubling with a waveguide PPLN pumped by an optical injection-locked diode laser," *Opt. Exp.*, vol. 18, no. 10, pp. 10308–10314, May 2010.
- [19] E. Kantola, T. Leinonen, S. Ranta, M. Tavast, and M. Guina, "High-efficiency 20 W yellow VECSEL," *Opt. Exp.*, vol. 22, no. 6, pp. 6372–6380, Mar. 2014.
- [20] T. Taira, W. M. Tulloch, and R. L. Byer, "Modeling of quasi-three-level lasers and operation of cw Yb:YAG lasers," *Appl. Opt.*, vol. 36, no. 9, pp. 1867–1874, Mar. 1997.
- [21] A. A. Kaminskii, *Laser Crystals: Their Physics and Properties*, 2nd ed. Berlin, Germany: Springer-Verlag, 1989.
- [22] D. H. Li, "Theoretical and experimental studies of noise suppression for intracavity frequency doubled lasers with phase matching type I or II," *Opt. Commun.*, vol. 189, no. 4–6, pp. 357–364, Mar. 2001.
- [23] B. Li, "A novel CW yellow light generated by a diode-end-pumped intra-cavity frequency mixed Nd:YVO₄ laser," *Opt. Laser Technol.*, vol. 56, pp. 99–101, Mar. 2014.